Article:
Yin, L. orcid.org/0000-0001-7148-0943, Cai, J., Ma, L. et al. (5 more authors) (2024) Dual function of magnetic nanocomposites-based SERS lateral flow strip for simultaneous detection of aflatoxin B1 and zearalenone. Food Chemistry, 446. 138817. ISSN 0308-8146

https://doi.org/10.1016/j.foodchem.2024.138817

Supplementary Material

Dual function of magnetic nanocomposites-based SERS lateral flow strip for simultaneous detection of aflatoxin B1 and zearalenone

Limei Yin[a,b]*, Jianrong Cai[b], Lixin Ma[b], Tianyan You[a], Muhammad Arslan[b], Heera Jayan[b], Xiaobo Zou[b], Yunyun Gong[c]*

[a] *International Joint Research Laboratory of Intelligent Agriculture and Agri-products Processing, School of Agricultural Engineering, Jiangsu University, Zhenjiang 212013, China*

[b] *China Light Industry Key Laboratory of Food Intelligent Detection & Processing, School of Food and Biological Engineering, Jiangsu University, Zhenjiang 212013, China*

[c] *School of Food Science and Nutrition, University of Leeds, Leeds LS2 9JT, UK*

*Corresponding author at: School of Food and Biological Engineering, Jiangsu University, Zhenjiang 212013, China

*Corresponding author at: School of Food and Biological Engineering, Jiangsu University, Zhenjiang 212013, China

Email address: yinlm6@163.com (L.M. Yin), Y.Gong@leeds.ac.uk (Y. Gong)

S1. Introduction

Many countries and organizations have established the maximum residue levels (MRL) of AFB1 and ZEN in corn, and the details are shown in Table S1.

Table S1. The maximum residue levels (MRL) of AFB1 and ZEN are defined by different countries and organizations.

Country or Organization	Sample	MRL (μg/kg)	
		AFB1	ZEN
China	corn and corn products	20	60
	baby grain food	0.5	60
European Union	unprocessed corn	5	300
	corn for direct human consumption	2	100
	baby grain food	0.1	20
America	corn and corn products	20	200
Japan	corn	10	20

S2. Experimental

S2.1 Chemicals and reagents

Chlorauric acid ($HAuCl_4 \cdot 4H_2O$), -(*N*-morpholino) ethanesulfonic acid (MES), tetramercaptobenzoic acid (4-MBA), *N*-hydroxysuccinimide (NHS), bovine serum albumin (BSA), 1-(3-dimethylaminopropyl)-3-ethylcarbodiimide hydro (EDC), 2, polyvinylpyrrolidone K30 (PVP K30), trehalose and Proclin 300 were purchased from Sigma-Aldrich (Shanghai, China). Ethylene glycol, polyethylene glycol 400 (PEG 400), anhydrous sodium acetate, Ferric chloride ($FeCl_3 \cdot 6H_2O$), polyethyleneimine branched (PEI, MW 25 kDa), sodium citrate dihydrate ($Na_3C_6H_5O_7 \cdot 2H_2O$), ascorbic acid (AA), Tween-20, silver nitrate ($AgNO_3$), were obtained from company of

Sinopharm Chemical Reagent LTD (Beijing, China). Powder of Phosphate buffered saline (PBS) (readily available) was acquired from the company of Shanghai Maclin Biochemical Technology Ltd. (China) and liquefied via ultrapure $H_2O$to offer PBS buffer solution (pH 7.4, 0.01 M). A Milli-Q water refinement apparatus was employed to get highly pure water (≥18.2 MΩ cm, Millipore, Milford, MA, USA) during the trials.

Standard solutions of AFB1, ZEN, DON, FB1 OTA, s AFB1-BSA, ZEN-BSA, mAbs, AFB1-mAb and ZEN-mAb were bought from Beijing Huaan Magnech Bio-Tech Co., Ltd. (Beijing, China). Rabbit immunoglobulin G (IgG) and goat anti-rabbit IgG were acquired from Beijing Solaibao Technology Co., LTD. (Beijing, China). CN 95 (15 μm pore dimension) and CN 140 (8 μm pore dimension) were provided by Sartorius (Germany). FF80HP with 18 μm pore size, sample pad (Fusion 5), absorbent pad (CF4) and PVC plastic board were obtained from GE Whatman (Shanghai, China). 96-well microwell plates were got from Jingan Biotechnology (Shanghai, China). Positive corn samples (contaminated with AFB1 and ZEN) were collected by Beijing Meizheng Testing Technology Co., LTD. (Beijing, China).

S2.2 Instruments

UV-vis absorbance bands of synthesized nanoparticles were documented by UV-1601 Spectrophotometer (Beifen-Ruili Ltd., Beijing). While TEM pictures were acquired via a JEM-200CX microscope (JEOL Ltd., Tokyo, Japan). Elemental composition of Au^{MBA}@Ag nanoparticles was characterized by scanning electron

microscopy (SEM) integrated with energy-dispersive X-ray spectroscopy (SEM-EDS, Hitachi Ltd., Japan). Elemental mapping images of Fe_3O_4@PEI/Au^{MBA}@Ag were chronicled by energy-dispersive X-ray spectroscopy (EDS) by means of a Philips Tecnai G2 F20 microscope equipped with a STEM unit. Additionally, Zeta potentials were obtained using a Malvern Nano-ZS90 system. The strips were prepared using the colloidal gold jet platform (Biodot XYZ 3060) and a programmable cutter (CM 4000). The Confocal Raman microscope (10× target and a boosting wavelength of 638 nm at 15 mW; XploRA PLUS, HORIBA, Paris, France) was employed to secure peaks of Raman. Raman spectra of test lines were taken from a handheld Raman spectrometer (HRS-5A; American Ocean Optics Co., Ltd., San Diego, CA, USA) with 785 nm laser excitation and a 100 μm diameter laser spot. An HPLC that emerged with a fluorescence detector (Shimadzu Corporation, Japan) was applied to detect the reference content of mycotoxins (AFB1 and ZEN) in corn samples. high-angle annular dark-field scanning transmission electron microscopy (HADDF-STEM)

S2.3 Preparation of Au-IgG

Initially, K_2CO_3 (80 μL, 0.2 M) was utilized to adjust pH of AuNPs solution (10 mL) to pH 8.5, next via sluggish stirring 500 μL of rabbit immunoglobulin G (IgG) (0.2 mg/mL) which was dissolved in PBS (0.01 M, pH 7.4), was combined with AuNPs solution. Half an hour later, BSA (1 mL, 1%) was added to the mixture to obstruct the residual sites. In the aftermath of 30 min, the supernatant was purified by centrifugation of the suspension for 10 min at 7800 g. Then PBS buffer (2 mL, 10

mM) involving 1% of each BSA and PVP, 0.05% Tween-20 as well as 2% sucrose was employed to resuspend the final precipitate.

S2.4 HPLC analysis of AFB1 and ZEN

The determination of AFB1 and ZEN in corn samples was carried out according to the HPLC-FLD method of Chinese standard GB 5009.22-2016 and GB 5009.209-2016 (He, et al., 2020; Liao, et al., 2021). Sample pretreatment steps are as follows: five grams of corn flour was placed in a 50 mL centrifuge tube and 20 mL of methanol/water extracting solution (80%, v/v) was added. Then, the mixture in the centrifuge tube was vigorously shaken on a vortex mixer for 5 min and centrifugated at 3800 g for 5 min. Afterward, 10 mL of supernatant was mixed with 40 mL of ultrapure water and the mixture was filtered through a glass fiber filter paper to collect the filtrate. Subsequently, 20 mL of filtrate (equivalent to 1 g corn) was passed through the immunoaffinity column (AFB1 or ZEN) slowly. Finally, the immunoaffinity column was eluted with 1 mL of methanol and the eluant was filtered through a 0.22 μm filter for HPLC detection.

A reverse-phase C18 HPLC column (4.6×250 mm and particle size equal to 5 μm) was used for the analysis. The conditions for liquid chromatography were as follows. AFB1 was determined using a fluorescence detector with post-column photochemical derivatization. The fluorescence detection was set as 360 nm for excitation and 440 nm for emission. The mobile phase consisted of a mixture of water/acetonitrile/methanol (60/20/20, v/v/v) with equal gradient elution and the flow

rate was at 1.0 mL/min. ZEN was determined using a fluorescence detector. The fluorescence detection was set as 274 nm for excitation and 440 nm for emission. The mobile phase consisted of a mixture of water/acetonitrile (50/50, v/v) with equal gradient elution and the flow rate was at 1.0 mL/min. Retention times of AFB1 and ZEN were found to be 15.842 min and 9.286 min. The calibration curves of AFB1 and ZEN were established by external standard methods for quantitive analysis.

S3. Results and Discussion

S3.1. Characterization of Au^{MBA}@AgNPs

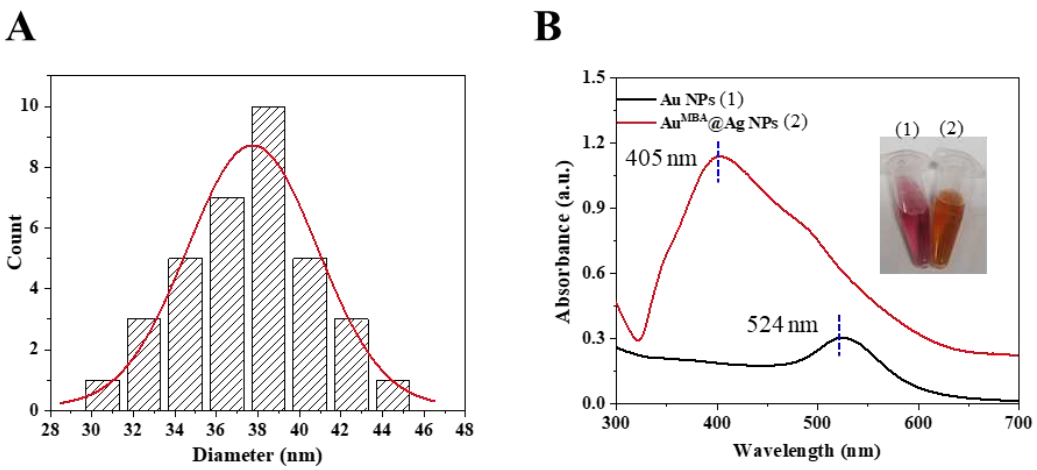

Fig. S1. (A) Particle size distribution of Au^{MBA}@AgNPs. (B) UV-vis spectra of AuNPs and Au^{MBA}@AgNPs; the inserted image is the photo of two colloidal solutions.

S3.2. Investigation of maximum load capacity

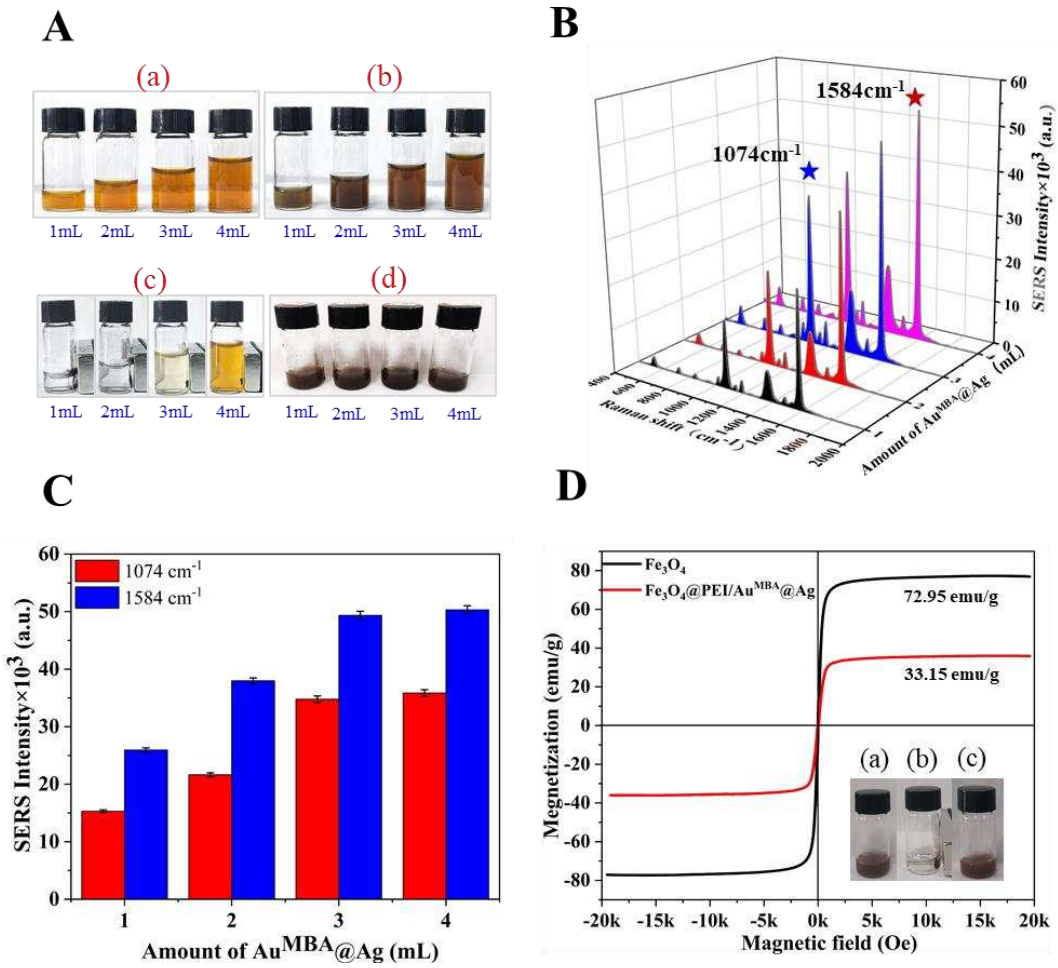

Fig. S2. (A) Experimental photographs of the adsorption of Au^{MBA}@AgNPs on Fe_3O_4@PEI. (B) Raman spectra of the resuspension of Fe_3O_4@PEI/Au^{MBA}@Ag tags (C) Raman intensities of characteristic peaks of Fe_3O_4@PEI/Au^{MBA}@Ag tags at 1074 cm^{-1} and 1584 cm^{-1}. (D) Magnetic hysteresis curves of Fe_3O_4 and Fe_3O_4@PEI/Au^{MBA}@Ag, and the inserted picture displayed the dispersion state of Fe_3O_4@PEI/Au^{MBA}@Ag solution before and after enrichment under an external magnetic field.

S3.3. Calculation of enhancement factor（EF）

To verify the SERS activity of the novel SERS tag (Fe_3O_4@PEI/Au^{MBA}@Ag), the SERS enhancement effect of two nanoparticles (Au^{MBA}@AgNPs and

Fe_3O_4@PEI/Au^{MBA}@Ag) was compared and their enhancement factors (EFs) was calculated using the following equation:

$$EF = \frac{I_{SERS}}{I_{NR}} \times \frac{C_{NR}}{C_{SERS}} \quad (1)$$

where I_{SERS} and I_{NR} represent the SERS intensity and normal Raman signal of 4-MBA at 1584 cm^{-1} in the presence and absence of SERS active substrates, whereas C_{SERS} and C_{NR} are the concentration of SERS and normal Raman scattering, respectively. As shown in Table S2, 4-MBA (0.1M) showed a faint Raman signal (363 a.u.) in the absence of enhanced substrate. After the 4-MBA was embedded in Au@Ag, the Raman signal was improved significantly (13838 a.u.) at the concentration of 10^{-6} M. This could be due to the location of the 4-MBA molecule at the junction of the Au core and the Ag shell, where the narrow gap could create a large electromagnetic field (Wang, et al., 2021). After the Au^{MBA}@Ag was adsorbed on the surface of the Fe_3O_4@PEI, the Raman intensity of the Fe_3O_4@PEI/Au^{MBA}@Ag (49357 a.u.) was further improved. As exhibited in Table S2, EFs of Au^{MBA}NPs and Fe_3O_4@PEI/Au^{MBA}@Ag were calculated as 3.81×10^6 and 4.53×10^7.

Table S2. The enhancement factors (EF) of two nanoparticles.

Substrate	*Ext (s)*	C_{NR}（M）	I_{NR}（a.u.）	C_{SERS}（M）	I_{SRES}（a.u.）	EF
4-MBA	1	0.1	363	/	/	/
Au^{MBA}@Ag	1	/	/	10^{-6}	13838	3.81×10^6
Fe_3O_4@PEI /Au^{MBA}@Ag	0.1	/	/	3×10^{-6}	49357	4.53×10^7

S3.4. HPLC detection results

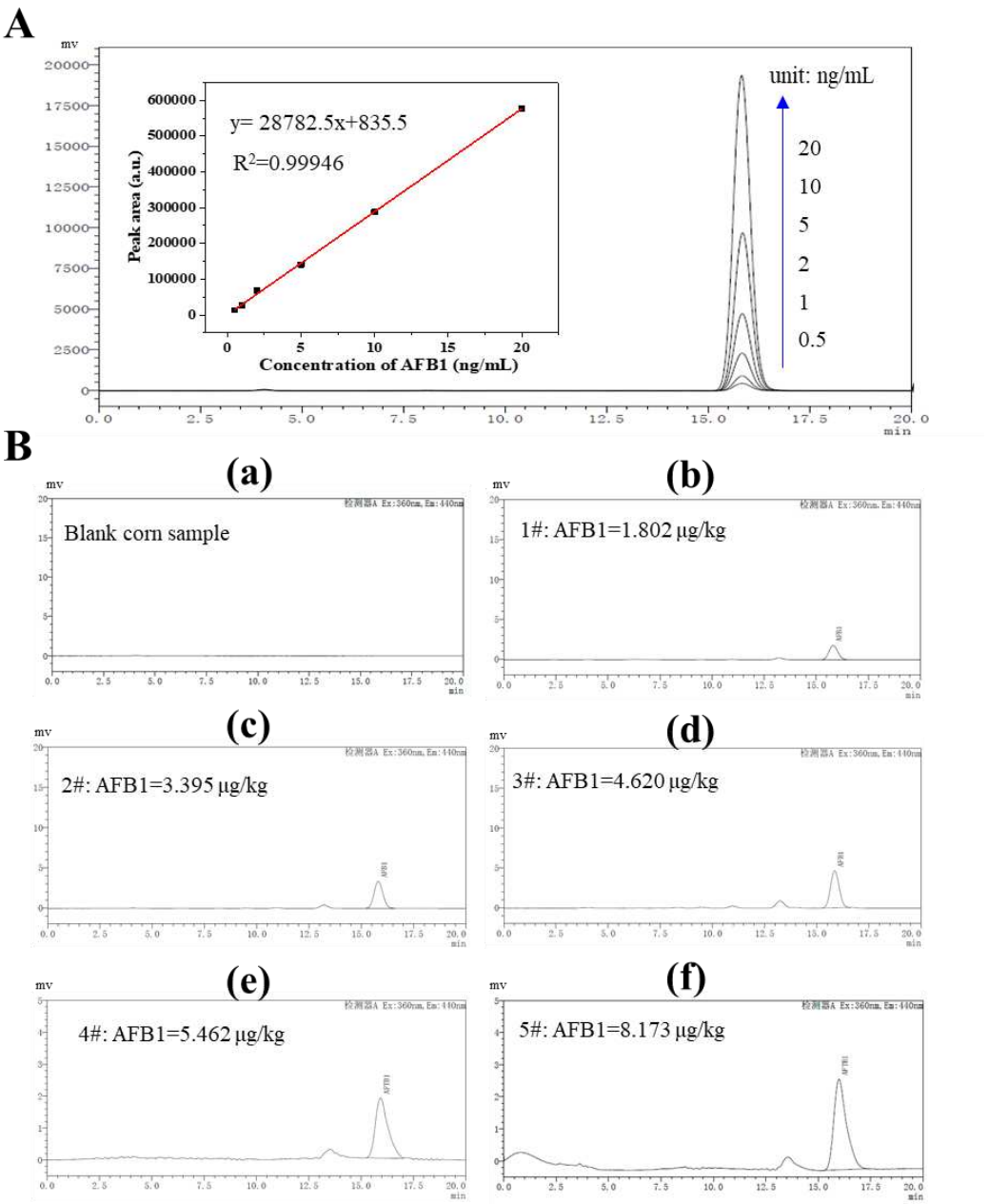

Fig. S3. (A) HPLC chromatogram of AFB1 standard solutions and the corresponding calibration curve. （B）HPLC chromatogram of blank corn sample (a) and several positive corn samples（b-f）.

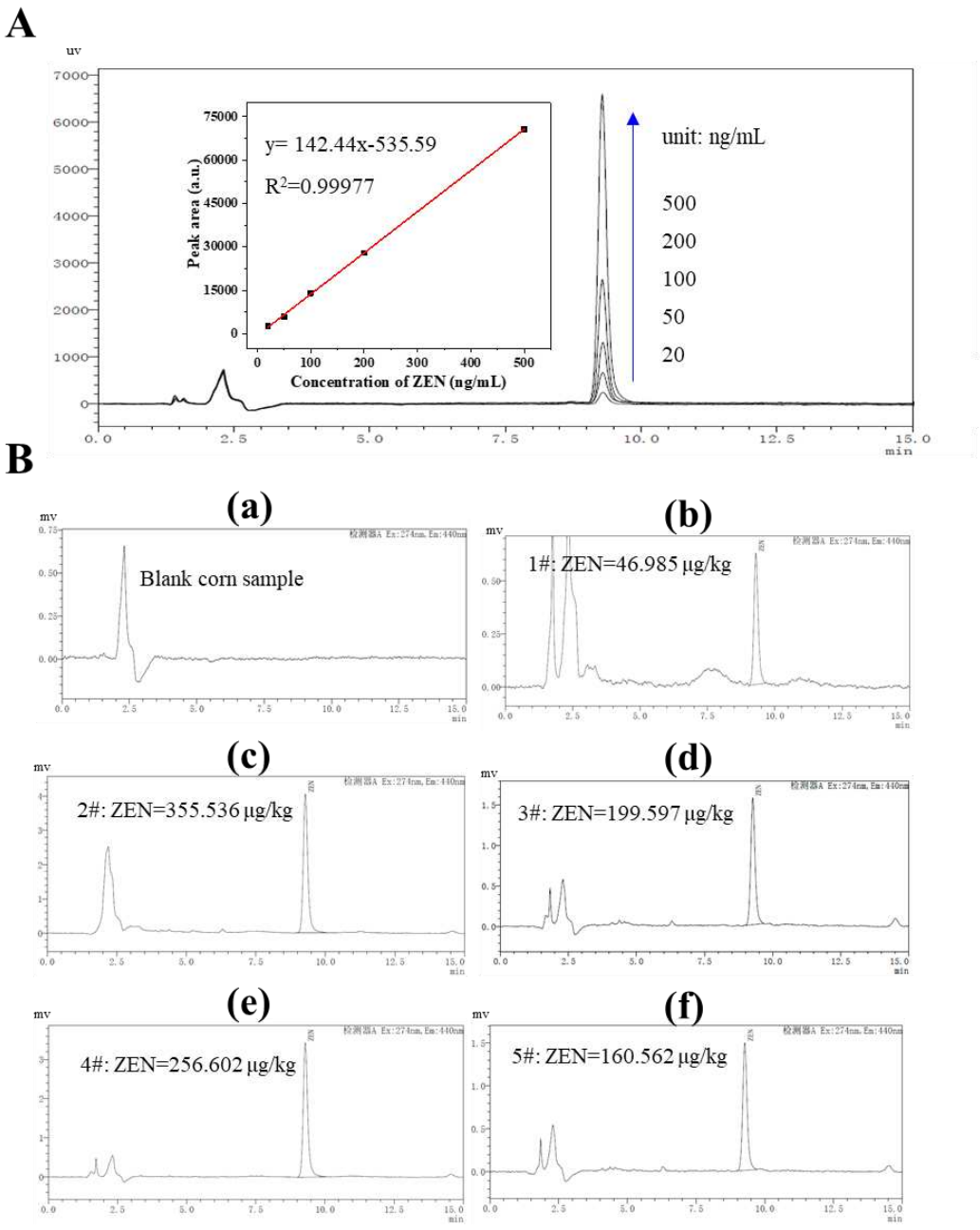

Fig. S4. (A) HPLC chromatogram of ZEN standard solutions and the corresponding calibration curve. （B）HPLC chromatogram of blank corn sample (a) and several positive corn samples（b-f）.

Table S3. Comparison of the present study and other SERS methods for multiple mycotoxins detection in corn.

Substrates	Technology	LODs of standard solution (ng/mL)	LODs of corn sample (μg/kg)	Recovery (%)	RSD(%)	Assay time (min)	Reference
3D-Nanocauliflower	SERS+label-free	AFB1: 1.8 ZEN: 47.7	AFB1: 3.6 ZEN: 95.4	94-110 97.8-104	/	~ 1	(Li, et al., 2019)
AuNPs on glass	SERS+IA	AFB1:0.066 ZEN: 0.57	AFB1:3.3 ZEN: 28.5	83.8-108.1	<15	80	(Li, et al., 2018)
MNPs@SSB+ AuNPs	SERS+aptasensor	AFB1:0.0052 ZEN: 0.00053	/	85.4-112.1	<7	70	(Yang, et al., 2022)
Au@Ag	SERS+LFIA	AFB1: 0.0014 ZEN: 0.015	AFB1: 0.14 ZEN: 1.5	83.2-106.2 78.9-97.3	<16	20	(Zhang, et al., 2020)
3D GO@Au-Au nanofilm	SERS+LFIA	AFB1: 0.00046 ZEN: 0.0046-10	AFB1: 0.0046 ZEN: 0.46	90.03-113.75	<13.48	20	(Zheng, et al., 2022)
Fe_3O_4@PEI/Au^{MBA}@Ag	SERS+LFIA	AFB1: 0.00476 ZEN: 0.095	AFB1: 0.0952 ZEN: 1.897	91.28-109.52 94.71-108.15	<10	20	This study

IA: immunoassay; LFIA: Lateral flow immunoassay; MNPs: magnetic nanoparticles; GO: graphene oxide; PEI: polyethyleneimine.

References

He, H., Sun, D.-W., Pu, H., & Huang, L. (2020). Bridging Fe_3O_4@Au nanoflowers and Au@Ag nanospheres with aptamer for ultrasensitive SERS detection of aflatoxin B1. *Food Chemistry, 324, 126832*. https://doi.org/10.1016/j.foodchem.2020.126832.

Li, J., Yan, H., Tan, X., Lu, Z., & Han, H. (2019). Cauliflower-Inspired 3D SERS Substrate for Multiple Mycotoxins Detection. *Analytical Chemistry, 91*(6), 3885-3892. https://doi.org/10.1021/acs.analchem.8b04622.

Li, Y., Chen, Q., Xu, X., Jin, Y., Wang, Y., Zhang, L., Yang, W., He, L., Feng, X., & Chen, Y. (2018). Microarray surface enhanced Raman scattering based immunosensor for multiplexing detection of mycotoxin in foodstuff. *Sensors and Actuators B: Chemical, 266*, 115-123. https://doi.org/10.1016/j.snb.2018.03.040.

Liao, Z., Yao, L., Liu, Y., Wu, Y., Wang, Y., & Ning, G. (2021). Progress on nanomaterials based-signal amplification strategies for the detection of zearalenone. *Biosensors and Bioelectronics: X, 9*, 100084. https://doi.org/10.1016/j.biosx.2021.100084.

Wang, L., Wang, X., Cheng, L., Ding, S., Wang, G., Choo, J., & Chen, L. (2021). SERS-based test strips: Principles, designs and applications. *Biosensors and Bioelectronics, 189*, 113360. https://doi.org/10.1016/j.bios.2021.113360.

Yang, Y., Su, Z., Wu, D., Liu, J., Zhang, X., Wu, Y., & Li, G. (2022). Low background interference SERS aptasensor for highly sensitive multiplex mycotoxin detection based on polystyrene microspheres-mediated controlled release of Raman reporters. *Analytica Chimica Acta, 1218, 340000*. https://doi.org/10.1016/j.aca.2022.340000.

Zhang, W., Tang, S., Jin, Y., Yang, C., He, L., Wang, J., & Chen, Y. (2020). Multiplex SERS-based lateral flow immunosensor for the detection of major mycotoxins in maize utilizing dual Raman labels and triple test lines. *Journal of Hazardous Materials, 393, 122348*. https://doi.org/10.1016/j.jhazmat.2020.122348.

Zheng, S., Wang, C., Li, J., Wang, W., Yu, Q., Wang, C., & Wang, S. (2022). Graphene oxide-based three-dimensional Au nanofilm with high-density and controllable hotspots: A powerful film-type SERS tag for immunochromatographic analysis of multiple mycotoxins in complex samples. *Chemical Engineering Journal, 448, 137760*. https://doi.org/10.1016/j.cej.2022.137760.